



# Structural condition assessment of a bridge pier: A case study using experimental modal analysis and finite element model updating

Qiang Mao<sup>1</sup> | Matteo Mazzotti<sup>1</sup> | John DeVitis<sup>2</sup> | John Braley<sup>2</sup> | Charles Young<sup>3</sup> | Kurt Sjoblom<sup>1</sup> | Emin Aktan<sup>1</sup> | Franklin Moon<sup>2</sup> | Ivan Bartoli<sup>4</sup> 

<sup>1</sup>Civil, Architectural and Environmental Engineering, Drexel University College of Engineering, Philadelphia, Pennsylvania, USA

<sup>2</sup>Department of Civil & Environmental Engineering School of Engineering, Rutgers, The State University of New Jersey, Piscataway, New Jersey, USA

<sup>3</sup>Intelligent Infrastructure Systems, Intelligent Infrastructure Systems, Pennoni Associates, Philadelphia, Pennsylvania, USA

<sup>4</sup>Civil, Architectural and Environmental Engineering, Drexel University, Philadelphia, Pennsylvania, USA

## Correspondence

Bartoli, Ivan, Civil Architectural and Environmental Engineering, Drexel University, Philadelphia, PA.  
Email: [ib77@drexel.edu](mailto:ib77@drexel.edu)

## Summary

Insufficient information on existing bridge substructures and foundations poses significant challenges for structural condition evaluation and can cause significant uncertainties for the safety and serviceability of bridges. Characterization and condition evaluation of bridges substructure and foundations will not only help to decrease the vulnerability to natural hazards but also provide opportunities for their reuse with considerable benefits. In this paper, the feasibility of leveraging structural identification techniques to characterize bridge substructures and foundations is investigated. A three-span simply supported bridge located in Mossy, West Virginia, USA, is used as a study case. Modal analysis and finite element model updating techniques are used to investigate and estimate the uncertainties and conditions of the substructure. Updated finite element model for this structure provides valuable information for bridge condition assessment and proves how structural identification is a viable tool for the case considered.

## KEYWORDS

bridge substructure, condition assessment, foundation, modal analysis, model updating, structural identification

## 1 | INTRODUCTION

The 2015 National Bridge Inventory included 614,387 structures (bridges and culverts) with a span greater than 20 ft (~6 m). Among them, 142,915 (23.3% of National Bridge Inventory) bridges have been identified as structurally deficient or functionally obsolete.<sup>1</sup> One of the major reasons for these bridges for being considered structurally deficient is insufficient documentation and information needed for a thorough structural condition evaluation. For instance, as of 2012, 36,076 bridges over waterways (riverine and tidal) are identified as having unknown foundations. Current practice evaluates bridge condition based on superstructure performance, but substructures and foundations also play an essential role in the load carrying capacity, dynamic performance, and serviceability of bridges.

Characterization and evaluation of the substructure of existing bridges is critical for bridge management and decision making for the several reasons. (a) Unknown foundations pose a great difficulty for condition evaluation and risk assessment of bridges. For example, foundation scour has been a major cause of bridge failures and still poses a significant threat to existing bridges.<sup>2</sup> Without knowing foundation information such as foundation type (shallow or deep),

depth of embedment, integrity, and settlement of foundations, the evaluation of the vulnerability of bridges to scouring problems is very difficult, if not impossible. (b) In addition, bridge foundation reuse could become a viable option in the replacement of structurally deficient superstructures, potentially providing technical, economic, time, and environmental benefits. Understanding the characteristics and condition of existing substructures should be prerequisite for making further decision on its reuse. (c) The final reason would be changes of service load and demand from superstructure. It is a common practice in the United States to undertake significant improvements on existing bridges (new decks, major rehabilitation, widening, and load capacity improvements) without in depth study of the current condition and remaining service life of the substructure, including the foundations.<sup>3</sup>

In this paper, structural identification (St-Id) techniques including modal analysis and finite element (FE) model updating will be leveraged to characterize and evaluate the substructure/foundation system of an existing bridge.

## 2 | BACKGROUND

The main factors of interest for bridge substructure characterization and evaluation include foundation embedded depth, foundation type, foundation material, foundation geometry, substructure integrity, substructure boundary condition, load bearing capacity of the substructure, scour vulnerability of the substructure, and remaining service life of substructure. To evaluate these parameters, many tools and technologies have been investigated, such as nondestructive evaluation (NDE), destructive testing, load testing, numerical modeling, geotechnical/geophysical site investigation, risk-based analysis, and statistical procedures. This section mainly concentrates on reviewing the application of NDE and structural identification.

NDE methods have been researched and implemented on bridge foundations by many research groups. Several studies summarize and discuss NDE techniques for characterization and evaluation of bridge substructures.<sup>4-9</sup> Among them, the National Cooperative Highway Research Program 21-5 project "Determination of Unknown Subsurface Bridge Foundations" and the National Cooperative Highway Research Program 21-5 (2) project "Unknown Subsurface Bridge Foundation Testing" provide a comprehensive review of technical literature and implementation of NDE approaches on substructure characterization.<sup>7,8</sup> The main NDE techniques leveraged for substructure characterization include Sonic Echo/Impulse Response/Bending Wave Method, Ultrasonic Method, Spectral Analysis of Surface Waves Method, Parallel Seismic Test Method, Borehole Sonic Test, Borehole Radar Method, Induction Field Method, and Ground Penetrating Radar. Of these, Borehole Parallel Seismic and Surface Ultra-Seismic methods are found to be the most accurate and broadly applicable borehole and surface methods.<sup>6</sup> There have been many successful implementations of these NDE methods on bridges in recent decades. Olson et al<sup>10</sup> evaluated the applicability of borehole-based NDE techniques for the determination of unknown subsurface bridge foundations. Huang and Chen<sup>11</sup> estimated the length of piles and the one-dimensional P-wave velocity in the pile using parallel seismic test. Huang and Ni<sup>12</sup> used several NDE techniques to detect defects in piles and to estimate the depth of deep foundations. Wang et al<sup>13</sup> showed the capability of electrical resistivity tomography for bridge foundation characterization. Nguyen et al<sup>14</sup> used surface-based seismic full waveform to evaluate existing foundations and successfully profiled embedded shaft elements and subsurface soil stratigraphy.

Although these NDE techniques have shown rapid development and significant achievement in the characterization of bridge substructure, they often still provide insufficient information to accurately evaluate the condition of the existing bridge substructure/foundation system. NDE techniques often focus on identifying local material or structural defects, rather than their influence on the global structural behavior and response which is also necessary to provide guidance for bridge management. Careful management strategy still requires understanding the structural effect of identified material deterioration, structural defects, and potential scour problems. Carefully designed field testing (including static and dynamic testing), reasonable load rating, and calibrated FE models should all be considered in an in depth substructure/foundation assessment strategy.

St-Id leverages civil engineering heuristics and field experiments in conjunction with analytical modeling for reliably characterizing constructed systems.<sup>15</sup> St-Id has demonstrated several advantages which could be extended to evaluate the condition of bridge substructure and bridge management. St-Id can be used to demonstrate the structural behavior and performance due to identified material deterioration, cracks/defects and foundation settlements, or rigid body rotation. A calibrated FE model as a product of St-Id can help bridge engineers reduce modeling errors, uncertainties, and unreasonable assumptions in the condition evaluation of existing foundations. The calibrated FE model can also be used for numerical simulations which will assist risk analysis and bridge management.

System identification techniques were first developed in the aerospace and automobile industry to verify and improve analytical models subsequently used in the simulation and design studies of the products. Halvorsen and Brown<sup>16</sup> discussed in detail the application of impulse techniques in experimental modal analysis to obtain frequency response measurements. Ibrahim<sup>17</sup> introduced a random decrement technique in the time domain to identify modal characteristics of structural systems. Liu and Yao<sup>18</sup> introduced the concept of system identification into civil/structural engineering as structural identification. Aktan et al<sup>19,20</sup> explained definition and terminology of structural identification. The analytical, experimental, and information tools for a successful St-Id of a constructed system were also discussed. St-Id has also been used for damage detection and identification as more modal parameter extraction methods and model updating algorithms were developed. Mottershead and Friswell<sup>21</sup> presented a comprehensive literature survey related to FE model updating, which has been used extensively for structural identification. Doebbling et al,<sup>22,23</sup> Farrar et al,<sup>24</sup> and Sohn et al<sup>25</sup> provided a comprehensive review of technical literature dealing with the detection, localization, and quantification of structural damage using vibration-based structural damage identification methods and model updating methods. Hearn and Testa<sup>26</sup> demonstrated modal analysis as a useful method for condition monitoring of bridges and other skeletal structures. Salawu<sup>27</sup> discussed the use of natural frequency as a diagnostic parameter in structural assessment procedures using dynamic vibration test. Ren et al<sup>28</sup> presented a practical and user-friendly FE model updating technique for constructed systems using ambient vibration test results. Gentile and Saisi<sup>29</sup> presented the results of the ambient-vibration-based investigations carried out to assess the structural conditions of a masonry bell-tower. Yang and Nagarajaiah<sup>30</sup> proposed an ICA-based time-frequency BSS framework for output-only modal identification for highly damped structures and tested it on laboratory experiment and real-measured seismic data. Behmanesh et al<sup>31</sup> proposed a hierarchical Bayesian model updating approach to estimate the inherent variability of structural parameters and implement probabilistic damage identification of structural systems. Noël and Kerschen<sup>32</sup> surveyed the key developments which arose in the field since 2006 and provided a broader perspective to nonlinear system identification by discussing the central role played by experimental models in the design cycle of engineering structures.

Many studies on bridge structures tend to emphasize St-Id of bridge superstructures with little consideration given to bridge substructure and their foundations. Fewer studies leverage dynamic properties or response characteristics of substructure obtained from field tests, small scaled model tests, and numerical models to characterize and evaluate bridge substructure. Maser et al<sup>33</sup> presented a method based on strain and rotation measurements which are used to compute a stiffness matrix for determining unknown foundation conditions. Olson<sup>34</sup> investigated the possibility to determine the condition and safety of the substructure and identify its foundation type by measuring the dynamic response characteristics of a bridge substructure. Samizo et al<sup>35</sup> proposed a practical method of quantitatively evaluating and assessing the structural integrity of bridge pier foundations in flood condition using natural frequencies obtained with microtremors. Manos et al<sup>36</sup> linked the variation of foundation dynamic characteristics to structural changes as well as soil–foundation interaction. Ko et al<sup>37</sup> used ambient vibration measurements on scaled bridge pier specimens to estimate structural integrity and foundation flexibility of a bridge pier. Sextos et al<sup>38</sup> studied the effect of soil conditions in the system identification process and investigated the efficiency of advanced FE modeling in representing the superstructure–soil–foundation stiffness with a scaled structure of a real bridge pier. Despite these attempts, there are very few studies using St-Id approach to identify the depth and boundary conditions of bridge substructure/foundation which are essential characteristics for condition evaluation. In this paper, St-Id approach is applied to the substructure of a steel multigirder bridge to investigate its feasibility on characterization and evaluation of bridge substructures. The study is performed on a real operating structure that while showing significant signs of deterioration remains crucial for the regional economy since is carrying large loading associated to nearby coal mining operations.

### 3 | DYNAMIC TESTING ON EXISTING SUBSTRUCTURE

The bridge selected for this test is the Mossy Interchange Bridge located in Mossy, West Virginia, USA, just off the West Virginia Turnpike (I-77). This bridge, which was built in 1954, is appraised as structurally deficient. This bridge serves several coal mines as an access point to the major highways in West Virginia, USA, so it undertakes considerable heavy truck traffic. It has three noncontinuous simply supported spans, which are composed of five steel stringers and a reinforced concrete slab. The center span is 51'9" long, and each of the side spans is 20'4" long. The bridge deck is 37'4" wide and serves two lanes. Figure 1 depicts the bridge and the two hammer head style piers. Pier 2 marked in the figure was selected as test specimen for characterization and evaluation.

Based on design drawings collected from the owner, the as built geometry of the pier is illustrated in Figure 2.



FIGURE 1 Mossy Interchange Bridge

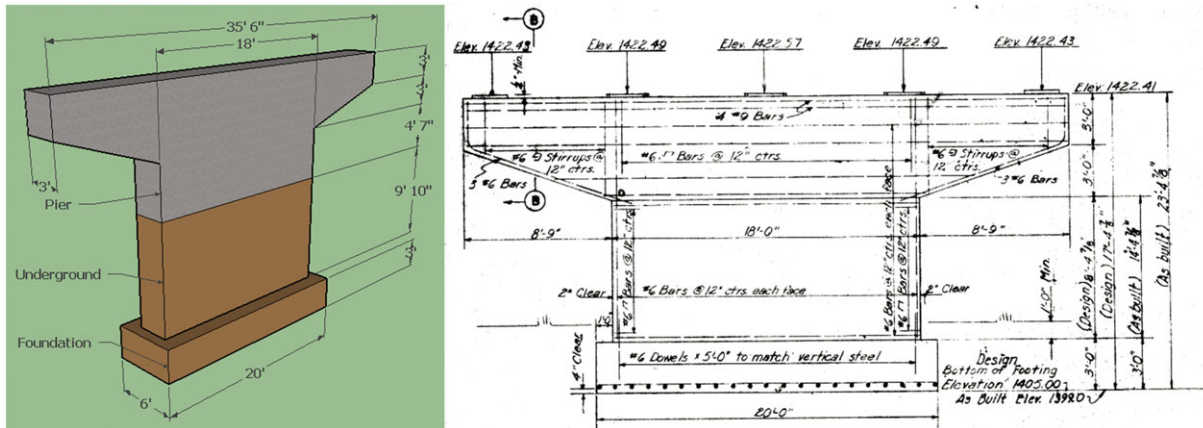
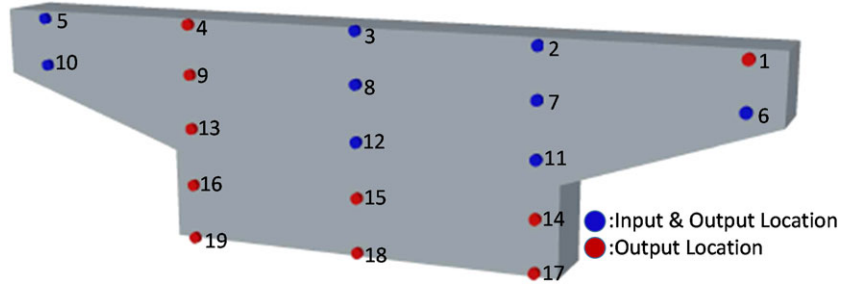


FIGURE 2 Pier 2 3D representation and original as-built plan

Pier 2 supports the center span and one side span with two sets of five steel bearings. As illustrated in the figure, the height of Pier 2 above the ground is 10'7", whereas the submerged depth is 9'10" according to as-built drawings. A strip footing with dimensions of 20' (length), 3' (depth), and 6' (width) supports the pier.

Multireference impact test (MRIT) was executed on Pier 2 to extract modal parameters. MRIT,<sup>39</sup> commonly used in field testing to extract modal parameters, can obtain reliable spatial modal response data with limited on-site instrumentation and operation. MRIT leverages multiple references and multiple outputs so that it provides repeated roots and differentiate close-spaced modes. Several impacts were imposed at each reference test point for data averaging to minimize random noise.

For MRIT, two instrumentation plans for accelerometers were designed to increase spatial resolution for the mode shapes extracted. The mode shapes extracted from both test plans will be combined together and then used for FE model calibration. Two sensors are selected as reference sensors for mode shape combination, and they are sensor 1, 2 in layout 1 (Figure 3), and sensor 19, 20 in layout 2 (Figure 4). The first sensor layout is designed to understand the overall vibration of the pier for each mode; in the meantime, the top two rows of sensors will help identify the condition of bearings on the pier top. The first layout of accelerometers is illustrated in Figure 3 and consists of 19



**FIGURE 3** Instrumentation plan 1 for Pier 2

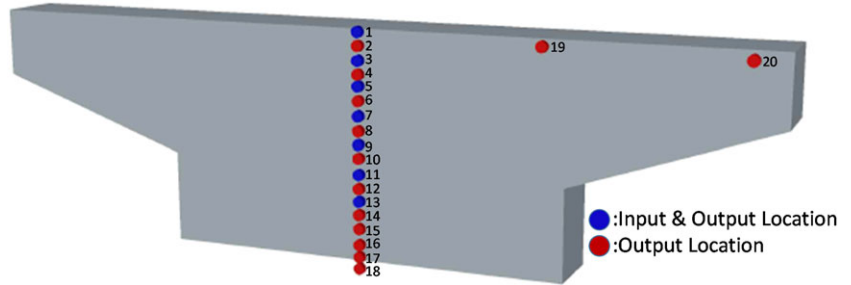


**FIGURE 4** Instrumentation plan 2 for Pier 2

accelerometers that were distributed on the surface of Pier 2. A total of seven locations were selected for impacts (blue dots in Figure 3). At each location, at least five impacts were performed for averaging purposes. The impact was conducted using an instrumented hammer PCB 086C42, outfitted with a hard tip and the accelerations were measured by uniaxial accelerometers, PCB 393A-03.

The second sensor layout is meant to identify the vibration along the center line of the pier under each mode and facilitate estimation of information for the underground part of the pier including embedded depth and soil-pier interaction. The second instrumentation plan arranged 18 accelerometers along one vertical line in the middle of the pier surface, as illustrated in Figure 4. For this layout, seven locations were selected for hammer impacts (blue dots in Figure 4). The sensor layouts for these two instrumentation plans on the tested pier can be seen in Figure 5.

#### 4 | TESTING RESULTS

The particular characteristics of an impulsive force signal and the resulting structural response signal make the MRIT especially susceptible to two problems: noise error and leakage problem. The duration of an impact is usually much smaller than the recorded time history, which may cause the total energy of the noise to be high compared with the energy of the impact. To alleviate this, the force window is set to unity over the time signal containing impact and zero at all the time history other than the impact because they are all electrical noise. To minimize the torsion effect of transformed signal from the sharp boundary of the unity window, two steep cosine tapers are used to connect unity to zero signal.



**FIGURE 5** Sensor layouts for the two instrumentation plans

Leakage refers to errors caused by deviations from the assumption that the signal is periodic within the sampling period. If the response signal does not decay to zero at the end of the time history, leakage error will occur and distort the Fourier transform. An exponential window is applied to response time history so that it will decay to near zero at the end of the time history. Because the nature of the structure's free response is also exponential, the effect of the response window is only an increase of the damping of the structure without altering the resonance frequencies and corresponding mode shapes.<sup>16</sup>

To extract modal information from MRIT results, the frequency response function (FRF) needs to be formulated from the MRIT input and output data. Three formulation methods can be used for estimation of FRF from experimental data, which comprised response DOF and a single input measurement at any one of the response DOFs<sup>40</sup>:

- H1 Algorithm: Minimize Noise on Output
- H2 Algorithm: Minimize Noise on Input
- Hv Algorithm: Minimize Noise on Input and Output

The FRF may be computed directly from the definition as the ratio of the Fourier transforms of the output and input signals. However, better results are obtained in practice by computing the FRF as the ratio of the cross-spectrum between the input and output to the auto-power spectrum of the input which is H1 Algorithm. The H1 algorithm, the most commonly used formulation of the FRF, is adopted in this work. The algorithm uses the following definitions for the auto-power spectra<sup>40</sup>:

$$GFF_{qq} = \sum_1^{N_{avg}} F_q F_q^*, \quad (1)$$

$$GXX_{pp} = \sum_1^{N_{avg}} X_p X_p^*, \quad (2)$$

and the cross-power spectra:

$$GXF_{pq} = \sum_1^{N_{avg}} X_p F_q^*, \quad (3)$$

$$GFX_{qp} = \sum_1^{N_{avg}} F_q X_p^*, \quad (4)$$

where  $X$  is the Fourier transform of system output  $x$ ,  $F$  is the Fourier transform of system input  $f$ ,  $F_q^*$  is complex conjugate of  $F_q$ , and  $N_{avg}$  represents the number of averages. Then the FRF in the H1 algorithm form can be expressed as follows:

$$H_{pq} = \frac{GXF_{pq}}{GFF_{qq}}. \quad (5)$$

The H1 algorithm will only minimize the effect of output measurement noise. To measure the correlation of input and output signal, or the effect of noise and nonlinearity to both signals, the coherence function is defined as follows<sup>16</sup>:

$$\gamma_{pq}^2(f) = \frac{|GXF_{pq}|^2}{GFF_{qq} * GXX_{pp}}. \quad (6)$$

According to the definitions of the auto-power spectrum and cross-power spectrum, the coherence function will be identically equal to 1 if there is no measurement noise and the system is linear. The minimum value of the coherence function, which occurs when the two signals are totally uncorrelated, is 0. Thus, the coherence function is a measure of the contamination of the two signals in terms of noise and nonlinear effects, with very low contamination indicated for values close to 1.

A typical FRF plot extracted from experimental data is shown in Figure 6 in terms of phase and FRF magnitude. The bottom plot in Figure 6 shows also the coherence function.

The complex mode indicator function (CMIF) combined with enhanced FRF (eFRF) is selected here for the data postprocessing. CMIF is based on eigenvalue decomposition (ED) or singular value decomposition (SVD) methods applied to multiple reference FRF measurements, and it can detect modes by picking the peak of ED or SVD curve plots especially for closely spaced or repeated modes.<sup>41</sup> The eigenvector or the left-side singular vector obtained from decomposition operation can then serve as a spatial filter to form eFRF from the FRF matrix. The process leverages the concept of transforming physical space to modal space so that one particular mode of vibration will be enhanced and problem will become to solving single degree-of-freedom (SDOF) modal problem. By selecting eFRF results from several frequency line around the selected peaks of CMIF, modal parameters include modal frequencies, modal damping, and modal scaling of a SDOF characteristic can be obtained through least square methods.

The generation of CMIF starts from the decomposition of the FRF matrix  $[H(w)]$ :

$$[H(w)] = [U(w)][\Sigma(w)][V(w)]^H = [\Psi] \left[ \frac{1}{j\omega_i - \lambda_r} \right] [L]^T. \quad (7)$$

$\omega_i$  is the  $i$ th frequency;  $\lambda_r$  is  $r$ th system pole;  $[\Psi]$  contains the modal vectors;  $[L]$  is the modal participation matrix, and each column  $\{L\} = Q_r\{\psi_{ar}\}$ ;  $\{\psi_{ar}\}$  is the modal vector at the driving points that represent the points where both input and output are measured;  $Q_r$  is modal scale factor for mode  $r$ .

It is known that the left and right singular vectors,  $[U]$  and  $[V]$ , have length 1 in the SVD formulation. In terms of the mode shapes and participation vectors,  $[\Psi]$  and  $[L]$  are constant for a particular mode. Therefore, along the frequency line near a resonance, the system pole  $\lambda_r$  and the input frequency  $\omega_i$  are closer, which result in a local maximum of the CMIF plot. The peak singular values at the CMIF plots are possible pole locations of the system. The left singular vector associated with the peak singular vector is the approximate modal vector of the system. The CMIF plot obtained for the test performed on Pier 2 is shown in Figure 7.

From the CMIF plot, the potential modes are selected with a peak picking criterion and marked with red circles (Figure 7). The first marked mode is at 0 Hz, and it is recognized as a computational mode. The last marked mode is at 400 Hz, and although it is identified by the peak picking criterion, it is also not a real mode for the pier. Several peaks are identified in the frequency range of 1 to 40 Hz which are not selected as modes because after plotting the deflected shapes at these frequencies and comparing the modal results from superstructure test, these peaks actually represent superstructure modes which will be discussed in the following.

A virtual measurement, known as the eFRF, is used to identify the modal frequencies and scaling of an SDOF characteristic that is associated with each peak in the CMIF. The eFRF is developed based upon the concept of physical to modal coordinate transformation and is used to manipulate FRFs so as to enhance a particular mode of vibration. The left singular vectors, associated with the peaks in the CMIF, can be used as an estimate of the modal filter which accomplishes this. The eFRF then can be expressed as follows<sup>42</sup>:

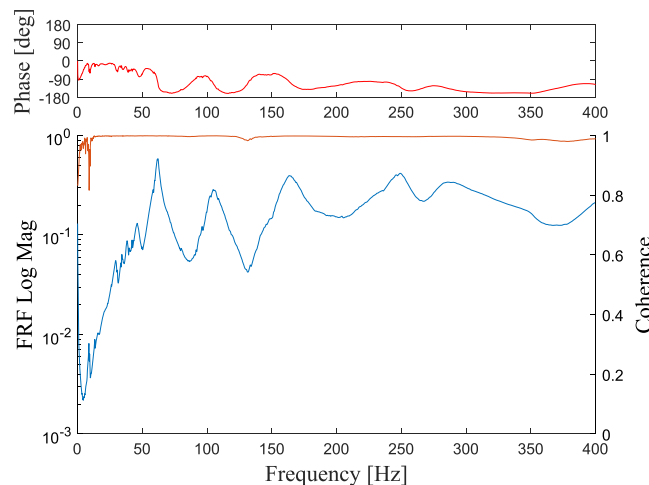


**FIGURE 6** Typical frequency response function plot

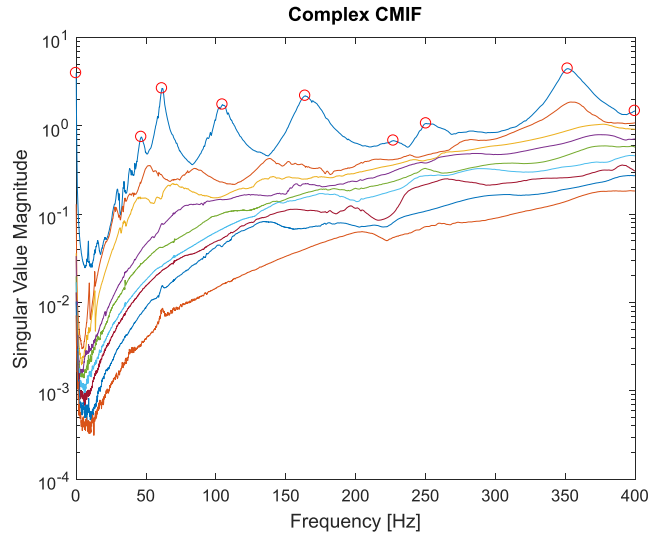


**FIGURE 7** Complex mode indicator function (CMIF) plot

$$eFRF_r(w) = \frac{Q_r}{(jw - \lambda_r)}, \quad (8)$$

where  $Q_r$  is modal scale factor for mode  $r$ .

After the eFRF is obtained, it is then used in the unified matrix polynomial approach<sup>43</sup> to perform a least squares curve fit of the temporal domain and obtain damping and natural frequency estimates for each mode. The simplified, second-order unified matrix polynomial approach model is the following:

$$\sum_{k=1}^n [\alpha_k](jw)^k eFRF_r(w) = \sum_{k=1}^n [\beta_k](jw)^k, \quad (9)$$

where  $[\alpha_k]$  and  $[\beta_k]$  are the coefficient matrices extracted using the least square method. Finally, the poles of the system can be determined on a mode by mode basis, and the modal scaling of the modal vectors can be computed.

One difficulty encountered when identifying substructure modes is differentiating them from superstructure modes. Because the peaks in the CMIF plot include all the modes for the entire bridge, the superstructure modes have to be sorted out. There are several factors considered here when selecting substructure modes. The first factor considered is the coherence function. As discussed before, when coherence is relative low in a frequency range, the modes identified and included in this region are likely to be associated with the superstructure modes rather than being fundamental substructure modes. Secondly, leveraging the dynamic testing operated directly on the superstructure, the identified superstructure modal peak frequencies can be ruled out from the peaks picked in the CMIF plot. Finally, frequency analysis results from a priori FE model can also help separating the mode shapes and frequencies associated with the superstructure and the substructure. This information facilitates the choice of substructure modes. Using these criteria, the mode shape and modal properties of the substructure were estimated and are shown in the Figure 8 and summarized in Table 1.

From the test performed using the second instrumentation plan, the mode shapes reconstructed with a vertical line of accelerometers (Figure 4) are also extracted. Four flexural modes match the results from the first instrumentation plan shown in Figure 9.

## 5 | FE MODEL CONSTRUCTION AND CALIBRATION

The preliminary a priori FE model is constructed through a FEM software package, COMSOL Multiphysics, and calibrated through Comsol Livelink with Matlab by minimizing the difference between FEM and experimental results.

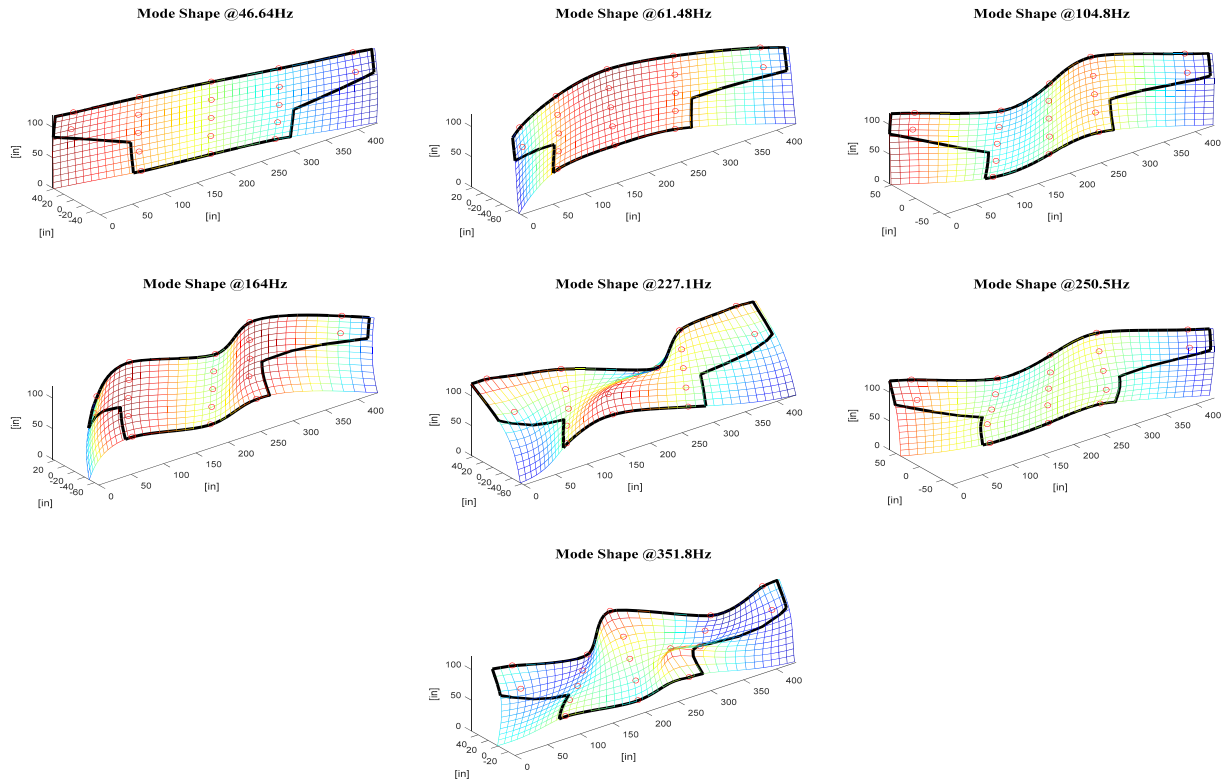


**FIGURE 8** Seven mode shapes extracted

**TABLE 1** Natural frequencies and damping for the seven modes

Mode	Frequency (Hz)	Damping (%)
1	46.64	10.79
2	61.48	4.04
3	104.8	3.50
4	164	1.96
5	227.1	2.50
6	250.5	1.23
7	351.8	0.46

This preliminary model (Figure 10) is constructed based on as-built plan and on site measurements and consists of the selected pier and the two spans directly supported on it. The pier is modeled with cubic Lagrange solid elements, whereas the deck, the girder webs, and flanges are represented by quadratic shell elements. The girders and deck are assumed to be rigidly connected. The two spans are supported by the bearings on the hammerhead pier top. The other ends of the spans are assumed to be simply supported. The bearings are modeled as restraints on the transversal and vertical direction and translational springs on the longitudinal direction of the beams. For the boundary condition of the pier and foundation, fixed restraints are assumed for the surface separating the bottom of the foundation and the soil. For the horizontal soil-pier/foundation interaction, a set of distributed springs perpendicular to the pier surface is defined.

This FE model is only a preliminary representation of the actual structure due to the uncertainties and assumptions associated with this it. To better refine the model, a calibration based on the modal parameters from dynamic testing is implemented. Usually, updating parameters are selected from geometry, material properties, boundary conditions, and inner joints and connections. As mentioned before, all the geometry information is known for the FE model. However, one of the objectives of this research is to investigate the possibility of leveraging experimental modal analysis to estimate the depth of the substructure/foundation system, so the depth is also considered as one updating parameter. Because it is already known through as-built plans, the updated value of the depth can also be used as a criterion to

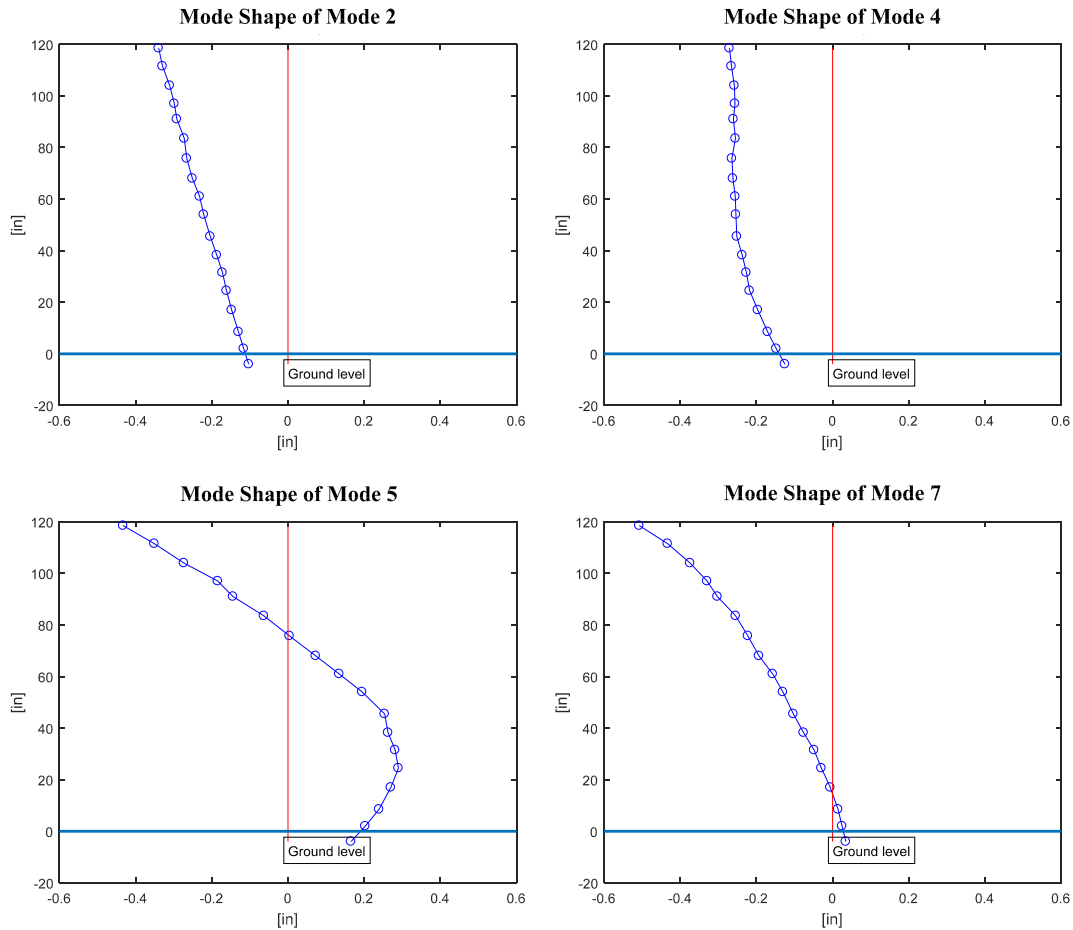


FIGURE 9 Mode shapes from second instrumentation plan

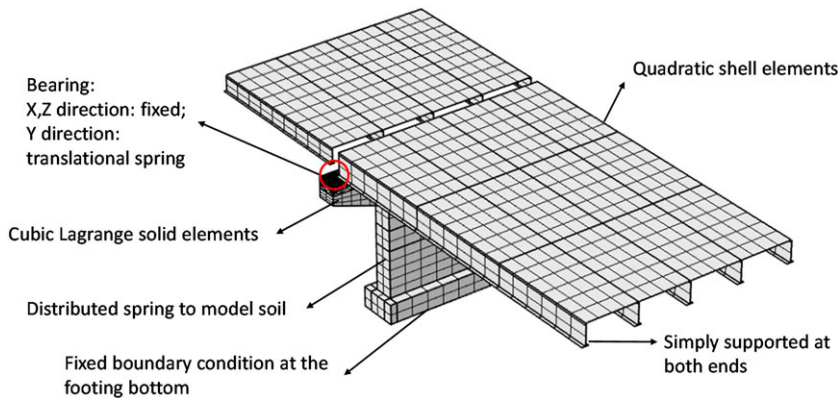


FIGURE 10 COMSOL model

assess the accuracy of model calibration process. The material properties of concrete are selected based on the results from NDE tests by ultrasonic surface wave equipment. Ten locations on the pier surface are selected, and for each location, three to five impacts are implemented with ultrasonic surface wave approach<sup>44</sup> yielding an estimate of the Young's modulus for the concrete. Material properties of steel have little variability and they are defined as listed in Table 2. The stiffness of the translational springs representing the bearing links between pier and superstructure and the distributed springs used for soil-pier interaction are assumed to have the initial values summarized in Table 3 and are included within the set of updating parameters.

Before calibrating the preliminary FE model, a sensitivity analysis is desirable for several reasons: (a) to determine the parameters that are more influential to the structure dynamic behavior and that consequently can be likely

**TABLE 2** Material properties used in the finite element model

Material	Density (lb/ft <sup>3</sup> )	Young's modulus (lb/ft <sup>2</sup> )	Poisson ratio
Concrete	156.07	6.266e8	0.2
Steel	486.94	4.177e9	0.3

**TABLE 3** Comparison of initial value and updated value of updated parameter coefficient

Updated parameter coefficient	Absolute number	Initial value	Updated value	Difference (%)
Foundation depth	7.28 (ft)	0.8	0.94	17.5
Distributed spring for soil pier interaction	6.366e7 (lb/ft/ft <sup>2</sup> )	1	0.1293	87.07
Translational spring for bearing 1	6.852e8 (lb/ft)	1	0.0150	98.50
Translational spring for bearing 2	6.852e8 (lb/ft)	1	0.0504	94.96
Translational spring for bearing 3	6.852e8 (lb/ft)	1	8.35E-06	100
Translational spring for bearing 4	6.852e8 (lb/ft)	1	0.0922	90.78
Translational spring for bearing 5	6.852e8 (lb/ft)	1	0.0088	99.12

**TABLE 4** Modal parameters comparison before and after model calibration

Mode	Natural frequency (Hz)						Mode shape (MAC)	
	Experimental	Initial		Updated		Initial	Updated	
		Analytical	Difference (%)	Analytical	Difference (%)			
1	46.64	84.64	81.48	46.67	0.06	0.9538	0.9757	
2	61.48	95.77	55.77	67.55	9.87	0.6645	0.9705	
3	104.8	134.95	28.77	104.8	0.00	0.9798	0.9258	
4	164	189.4	15.49	161.3	1.65	0.9657	0.9618	
5 <sup>a</sup>	227.1	249.06	9.67	218	4.01	0.8796	0.3543	
6 <sup>a</sup>	250.5	256.4	2.36	248.6	0.76	0.9363	0.9525	

<sup>a</sup>Not used in the calibration process.

extracted from the experimental modal analysis and (b) to determine the fitness function to be minimized that is more appropriate for the updating process. In this research, the fitness function used includes the normalized modal difference,<sup>45</sup> and it is defined as follows:

$$fitness = \frac{1}{n} \sum_{i=1}^n \alpha_i \left| \frac{f_i^e - f_i^a}{f_i^e} \right| + \frac{1}{n} \sum_{i=1}^n \beta_i NMD_i, \quad (10)$$

$$NMD_i = NMD(\{\phi_i^a, \phi_i^e\}) = \sqrt{\frac{1 - MAC_{ii}}{MAC_{ii}}}, \quad (11)$$

$$MAC_{ii} = MAC(\{\phi_i^a, \phi_i^e\}) = \frac{|\phi_i^a T \cdot \phi_i^e|^2}{\phi_i^a T \cdot \phi_i^e \cdot \phi_i^e T \cdot \phi_i^a}, \quad (12)$$

where  $f_i^e$  and  $f_i^a$  represent the analytical and experimental resonance frequencies, respectively, of the  $i^{th}$  mode;  $\phi_i^a$  and  $\phi_i^e$  are the analytical and experimental mode shapes, respectively, of the  $i^{th}$  mode;  $MAC_{ii}$  is the modal assurance criterion (MAC) value<sup>46</sup> calculated for  $\phi_i^a$  and  $\phi_i^e$ ; finally,  $\alpha_i$  and  $\beta_i$  are the weighting factors used in the objective function related

to the frequencies and the mode shapes, respectively. The weighting factors are selected based on the reliability of the modal parameters extracted from the experimental results. Considering that several modes extracted experimentally are in a relative high frequency band, the accuracy of their modal parameters (especially mode shapes) is not sufficient to assign a large weight. As a consequence, in this paper, only the first four modes are selected for the FE model updating.

The updating process is facilitated leveraging the Optimization Toolbox of MATLAB.<sup>47</sup> During the process, mode pairing based on MAC is performed at each iteration before calculating the fitness function to ensure that the same modes from experimental and analytical results are compared. The comparison between the parameters assumed in the preliminary FE model and the updated parameters used in the calibrated FE model is presented in Table 3.

The difference between the frequencies and mode shapes obtained from the updated FE model and estimated using the experimental modal analysis clearly decreases after model updating (Table 4). Also, even though only the first four modes are selected for FE model updating, the calibrated FE model still yields better frequency at the fifth and sixth modes, but the MAC value drops after the model calibration.

## 6 | RESULTS AND CONCLUSION

Dynamic testing including MRIT were implemented on a steel multigirder bridge substructure to extract modal features, to allow the calibration of a preliminary FE model built in COMSOL, and finally to characterize and assess the condition of the bridge substructure.

Several challenges were encountered in the experimental extraction of the modal parameters and in the separation of the modal properties characterizing the behavior of the substructure and the superstructure respectively. Usually, the frequencies obtained from the superstructure are in a lower frequency range; the mode shapes show smaller damping, so higher kinetic energy is stored in the superstructure from the excitation provided by traffic loading. In addition, when the superstructure modes are closely spaced to the substructure modes, it can be difficult to parse them by only modes detection techniques. Coherence from MRIT, the use of modal parameters extracted from the superstructure testing and the modal parameters estimated from preliminary FE model can help in identifying substructure modes and to isolate them from superstructure modes.

In this paper, leveraging COMSOL and MATLAB toolbox, the a priori FE model is calibrated seeking a satisfactory match between experimental modal parameters and FEM results. Several influential variables affecting the substructure dynamic behavior were updated including the pier height that was known from as built drawings. This parameter was used to check the quality of the updating process. The estimated depth of the foundation is approximately 6% shorter than the depth from as-built plan. In addition, although only the first four modes were used in the update process, the modal frequencies of modes 5 and 6 are very close to the experimental results. Finally, the stiffness associated to the center bearing (bearing no. 3, see Table 3) are very low which is consistent with the visual inspection of the supports that showed as the central bearing act as a floating bearing.

The St-Id described in this paper focused on the bridge foundation/substructure. The paper showed the potential of MRIT dynamic testing as a tool to characterize the bridge substructure and model it with a calibrated FE model accounting for superstructure/substructure interaction and foundation/soil interaction. This approach could be leveraged to assess the condition of the foundation/substructure system of existing bridges with limited documentation once its limitations and challenges are properly understood. It should be noted that the soil surrounding the foundation (including the soil under the footing bottom) remains a source of considerable uncertainty and introduces large damping. Consequently, future work is recommended on leveraging different modal analysis algorithms and modeling strategies to carefully account for the large damping. Furthermore, soil properties could be better studied by investigating modes at higher frequencies or combining the experimental modal analysis with appropriate NDE strategies.

## ORCID

Ivan Bartoli  <http://orcid.org/0000-0002-6038-8946>

## REFERENCES

1. FHWA. Bridge-tables of frequently requested NBI information. Washington, DC, accessed on 2016. Retrieved from <http://www.fhwa.dot.gov/bridge/britab.cfm> 2015

2. Melville BW, Coleman SE. *Bridge Scour*. Water Resources Publication; 2000.
3. Collin, J. G., & Jalinoos, F. Foundation Characterization Program (FCP): TechBrief# 1—Workshop Report on the Reuse of Bridge Foundations. Retrieved from 2014
4. Hossain M, Khan M, Hossain J, Kibria G, Taufiq T. Evaluation of unknown foundation depth using different NDT methods. *J. Perform. Constr. Facil.* 2011;27(2):209-214.
5. Niederleithinger, E., Wiggenhauser, H., & Taffe, A.. The NDT-CE Test and Validation Center in Horstwalde *Proceedings of NDTCE*, 9. 2009
6. Olson, L. (2002). Determination of Unknown Bridge Foundation Depths With NDE Methods. Paper presented at the First International Conference on Scour of Foundations.
7. Olson LD, Aouad MF. *Unknown Subsurface Bridge Foundation Testing*. Olson Engineering, Incorporated; 2001.
8. Olson LD, Jalinoos F, Aouad MF. *Determination of Unknown Subsurface Bridge Foundations*. Olson Engineering, Incorporated; 1995.
9. Rausche F. Non-Destructive Evaluation of Deep Foundations. Paper presented at the Proceedings of the Fifth International Conference on Case Histories in Geotechnical Engineering, New York. 2004
10. Olson LD, Liu M, Aouad MF. Borehole NDT Techniques for Unknown Subsurface Bridge Foundation Testing. Paper presented at the Nondestructive Evaluation Techniques for Aging Infrastructure and Manufacturing. 1996
11. Huang D-z, Chen L-z. Studies on parallel seismic testing for integrity of cemented soil columns. *J Zhejiang Univ Sci A*. 2007;8(11):1746-1753.
12. Huang Y-H, Ni S-H. Experimental study for the evaluation of stress wave approaches on a group pile foundation. *NDT & E Int.* 2012;47:134-143.
13. Wang H, Hu C-H, Wang C-Y. Electrical resistivity tomography to inspect bridge foundations. Paper presented at the Proceedings of the 3rd International Conference on Geotechnique, Construction Materials, and Environment (GEOMATE 2013). 2013
14. Nguyen TD, Tran KT, McVay M. Evaluation of unknown foundations using surface-based full waveform tomography. *J. Bridg. Eng.* 2016;21(5):04016013.
15. Catbas F, Kijewski-Correa T, Aktan A. Structural Identification (St-Id) of Constructed Facilities—Approaches, Methods and Technologies for Effective Practice of St-Id. Paper presented at the Am Soc Civ Eng. 2011
16. Halvorsen WG, Brown DL. Impulse technique for structural frequency response testing. *Sound Vib.* 1977;11(11):8-21.
17. Ibrahim S. Random decrement technique for modal identification of structures. *J. Spacecr. Rocket.* 1977;14(11):696-700.
18. Liu S-C, Yao JT. Structural identification concept. *J. Struct. Div.* 1978;104(12):1845-1858.
19. Aktan AE, Farhey DN, Brown DL, et al. Condition assessment for bridge management. *J. Infrastruct. Syst.* 1996;2(3):108-117.
20. Aktan AE, Farhey DN, Helmicki AJ, et al. Structural identification for condition assessment: experimental arts. *J. Struct. Eng.* 1997;123(12):1674-1684.
21. Mottershead J, Friswell M. Model updating in structural dynamics: a survey. *J Sound Vib.* 1993;167(2):347-375.
22. Doebbling S, Farrar C, Prime M, Shevitz D. Damage identification in structures and mechanical systems based on changes in their vibration characteristics: a detailed literature survey. *Los Alamos National Laboratory Rep. No. LA-13070-MS*. 1996
23. Doebbling SW, Farrar CR, Prime MB. A summary review of vibration-based damage identification methods. *Shock Vibration Digest.* 1998;30(2):91-105.
24. Farrar CR, Doebbling SW, Nix DA. Vibration-based structural damage identification. *Philosophical Trans Royal Soc London Series a: Mathematical, Phys Eng Sci.* 2001;359(1778):131-149.
25. Sohn H, Farrar CR, Hemez FM, et al. *A Review of Structural Health Monitoring Literature: 1996–2001*. NM: Los Alamos National Laboratory Los Alamos; 2004.
26. Hearn G, Testa RB. Modal analysis for damage detection in structures. *J. Struct. Eng.* 1991;117(10):3042-3063.
27. Salawu O. Detection of structural damage through changes in frequency: a review. *Eng Struct.* 1997;19(9):718-723.
28. Ren W-X, Zhao T, Harik IE. Experimental and analytical modal analysis of steel arch bridge. *J. Struct. Eng.* 2004;130(7):1022-1031.
29. Gentile C, Saisi A. Ambient vibration testing of historic masonry towers for structural identification and damage assessment. *Construct Build Mater.* 2007;21(6):1311-1321.
30. Yang Y, Nagarajaiah S. Time-frequency blind source separation using independent component analysis for output-only modal identification of highly damped structures. *J. Struct. Eng.* 2012;139(10):1780-1793.
31. Behmanesh I, Moaveni B, Lombaert G, Papadimitriou C. Hierarchical Bayesian model updating for structural identification. *Mech. Syst. Signal Process.* 2015;64:360-376.
32. Noël J-P, Kerschen G. Nonlinear system identification in structural dynamics: 10 more years of progress. *Mech. Syst. Signal Process.* 2017;83:2-35.

33. Maser KR, Sanayei M, Lichtenstein A, Chase SB. Determination of Bridge Foundation Type From Structural Response Measurements. Paper presented at the Non-Destructive Evaluation Techniques for Aging Infrastructure & Manufacturing. 1998
34. Olson L. Dynamic bridge substructure evaluation and monitoring (Report no. FHWA-RD-03-089). Retrieved from 2005
35. Samizo M, Watanabe S, Fuchiwaki A, Sugiyama T. Evaluation of the structural integrity of bridge pier foundations using microtremors in flood conditions. *Quarterly Report of RTRI*. 2007;48(3):153-157.
36. Manos G, Pitilakis K, Sextos A, Kourtides V, Soulis V, Thauampthep J. Field experiments for monitoring the dynamic soil–structure–foundation response of a bridge-pier model structure at a test site. *J. Struct. Eng.* 2014;141(1). D4014012
37. Ko Y-Y, Chang W-K, Liu K-Y, Hung H-H, Chang K-C. Damage evaluation for RC bridge piers using vibration measurement. *Adv Struct Eng.* 2015;18(9):1501-1515.
38. Sextos A, Faraonis P, Zabel V, Wuttke F, Arndt T, Panetsos P. Soil–bridge system stiffness identification through field and laboratory measurements. *J. Bridg. Eng.* 2016;21(10):04016062.
39. Fladung WA. The Development and Implementation of Multiple Reference Impact Testing. University of Cincinnati, 1994
40. Catbas FN. Identification of Global Condition Assessment and Structural Damage Identification of Bridges with Dynamic Testing and Modal Analysis. (PhD), University of Cincinnati, 1997
41. Shih C, Tsuei Y, Allemang R, Brown D. Complex mode indication function and its applications to spatial domain parameter estimation. *Mech. Syst. Signal Process.* 1988;2(4):367-377.
42. Allemang R, Brown D. A complete review of the complex mode indicator function (CMIF) with applications. Paper presented at the Proceedings, international conference on noise and vibration engineering (ISMA), Katholieke Universiteit Leuven, Belgium. 2006
43. Allemang R, Phillips A. The Unified Matrix Polynomial Approach to Understanding Modal Parameter Estimation: An Update. Paper presented at the Proceedings of ISMA International Conference on Noise and Vibration Engineering, Katholieke Universiteit Leuven, Belgium. 2004
44. Celaya M, Young G, Nazarian S. Portable Seismic Property Analyzer: Identification of Asphalt Pavement Layers: US Department of Transportation, Federal Highway Administration, Central Federal Lands Highway Division. 2009
45. Waters TP. Finite Element Model Updating using Measured Frequency Response Function. (PhD Thesis (PhD)), University of Bristol, England. 1995
46. Allemang, R. J., & Brown, D. L.. A correlation coefficient for modal vector analysis. Paper presented at the Proceedings of the 1st international modal analysis conference. 1982
47. Mathworks, T. *MATLAB&SIMULINK user's guide: MATLAB release 2006*. Natick, MA, USA: The Mathworks, Inc.; 2006.

**How to cite this article:** Mao Q, Mazzotti M, DeVitis J, et al. Structural condition assessment of a bridge pier: A case study using experimental modal analysis and finite element model updating. *Struct Control Health Monit.* 2019;26:e2273. <https://doi.org/10.1002/stc.2273>